DOI: 10.1002/chem.200800968

Ancillary Ligands and Spectator Cations as Controlling Factors in the Construction of Coordination and Hydrogen-Bonded Networks with the *tert*-Bu-C≡C⊃Ag_n ($n=4$, 5) Supramolecular Synthon

Liang Zhao, Chong-Qing Wan, Jie Han, Xu-Dong Chen, and Thomas C. W. Mak[a]

This work is dedicated to the memory of Professor Ao-Qing Tang (1915–2008)

Abstract: Supramolecular networks constructed with the *t*Bu−C≡C⊃Ag_n ($n=4$ or 5) metal–ligand synthon and trifluoroacetate have been transformed through the introduction of ancillary terminal nitrile ligands, from acetonitrile through propionitrile to *tert*-butyronitrile, giving rise to a 2D coordination network in AgC≡C*t*Bu·3 $AgCF_3CO_2$·H_2O (**1**), a 2D hydrogen-bonded network in AgC≡C*t*Bu·5 $AgCF_3CO_2$·4 CH_3CN·H_2O (**2**), a 2D hybrid coordination/hydrogen-bonded network in AgC≡C*t*Bu·3 $AgCF_3CO_2$·CH_3CH_2CN·2 H_2O (**3**), and another 2D coordination network in AgC≡C*t*Bu·4 $AgCF_3CO_2$·$(CH_3)_3CCN$·2 H_2O (**4**). Concomitantly, the linkage modes between adjacent ethynide-bound Ag_n aggregates in these compounds are also changed. A layer-type hydrogen-bonded host lattice in isostructural AgC≡C*t*Bu·4 $AgCF_3CO_2$·$(R_4N)(CF_3CO_2)$·2 H_2O ($R_4=BnMe_3$, **5**; $R_4=Et_4$, **6**; $R_4=nPr_4$, **7**) is obtained by introducing quaternary ammonium cations as guest templates, which occupy the interstices and thereby mediate the interlayer separation. Use of the bulky nBu_4N^+ cation leads to disruption of the host network in AgC≡C*t*Bu·4 $AgCF_3CO_2$·3-$[(nBu_4N)(CF_3CO_2)]$·H_2O (**8**) with generation of a discrete dense *nido*-Ag_5 cluster.

Keywords: alkyne ligands · host–guest systems · layered compounds · silver · supramolecular networks

Introduction

Since the mid-1980s, transition metal alkynyl complexes have been studied actively because their linear coordination geometry, high stability, and π-electron conjugation point to potential applications as precursors of nonlinear optical materials,[1] luminescence materials,[2] and rigid-rod molecular wires,[3] which involve not only complexes with just one alkynyl group bound to the metal but also coordination polymers that contain as many as a thousand M−C≡C− linkages in the polymeric chain −[M−C≡C−Y−C≡C]$_n$− (Y = aromatic spacer).[4] From the coordination chemistry viewpoint, transition metal alkynyl complexes can be regarded as derived from the prototypical HC≡C$^-$ ligand, which is isoelectronic with cyanide (CN^-), behaving as a good σ donor and modest π acceptor. The electronic characteristics of alkynyl ligands have also been investigated in some detail using spectroscopic and other structural techniques.[4a,5] In addition, the ethynide ligand can function as a good π donor through pπ–dπ overlap with metal atoms to engender a series of cluster complexes and multinuclear aggregates.[6]

Apart from the plethora of discrete metal alkynyl complexes whose bonding modes range from simple μ_1 to relatively complicated μ_4 types,[7] our recent studies on silver(I) complexes containing ethynide and perfluorocarboxylate ligands have demonstrated that the resulting polynuclear silver–ethynide aggregate,[8] symbolized by R−C≡C⊃Ag_n (R = alkyl or aryl, $n=4$ or 5), can be employed as a new kind of metal–ligand supramolecular synthon[9] in the construction of coordination networks. On the other hand, much effort has been concentrated on prediction and control of the formation of supramolecular networks by tuning various subtle factors, which commonly include the coordination preference of the central metal ion, the size and

[a] L. Zhao, C.-Q. Wan, J. Han, X.-D. Chen, Prof. Dr. T. C. W. Mak
Department of Chemistry and Center of Novel Functional Molecules
The Chinese University of Hong Kong, Shatin, New Territories
Hong Kong SAR (Peoples Republic of China)
Fax: (+852) 2603-5057
E-mail: tcwmak@cuhk.edu.hk

Supporting Information for this article (refinement details for the X-ray structural analysis) is available on the WWW under http://dx.doi.org/10.1002/chem.200800968.

shape of the ligands, the metal-to-ligand ratio, the rational arrangement of the supramolecular synthon, the nature of the counter-anion, and the solvents used in crystallization.[10] In contrast, the role of ancillary ligands in manipulating supramolecular assembly in crystalline solids is rarely investigated. In the present work, we utilize nitrile ligands as additional components in the synthesis to induce the formation of different coordination skeletons constructed with the *t*Bu-C≡C⊃Ag_n ($n=4$ or 5) supramolecular synthon and trifluoroacetate. Through variation of the steric bulk of added nitrile ligands, a series of silver(I) complexes, namely AgC≡C*t*Bu·3 $AgCF_3CO_2$·H_2O (**1**) and AgC≡C*t*Bu·n $AgCF_3CO_2$·m RCN·x H_2O (**2**, R = CH_3–, $n=5$, $m=4$, $x=1$; **3**, R = CH_3CH_2–, $n=3$, $m=1$, $x=2$; **4**, R = $(CH_3)_3C$–, $n=4$, $m=1$, $x=2$) has been synthesized and structurally characterized. We have also investigated the inclusion properties of the supramolecular host network in three isostructural complexes, AgC≡C*t*Bu·4 $AgCF_3CO_2$·(R_4N)(CF_3CO_2)·2 H_2O (**5**, R_4 = $BnMe_3$ where Bn = benzyl; **6**, R_4 = Et_4; **7**, R_4 = nPr_4), as well as the generation of a discrete dense *nido*-Ag_5 cluster in AgC≡C*t*Bu·4 $AgCF_3CO_2$·3 [($n$$Bu_4N$)($CF_3CO_2$)]·$H_2O$ (**8**), which are obtained with quaternary ammonium cations serving as guest templates.

Results and Discussion

We have previously reported the synthesis of the polymeric complex [*t*BuC≡CAg]$_n$ via the reaction of silver nitrate with equimolecular lithium *tert*-butylethynide (generated in situ from *tert*-butylacetylene and *n*BuLi) in THF under an inert atmosphere of nitrogen at room temperature.[8b] We subsequently utilized a concentrated aqueous solution of $AgCF_3CO_2$ and $AgBF_4$, the latter being added to increase the silver(I) ion concentration[11] requisite for dissolving [*t*BuC≡CAg]$_n$, thus ensuring the formation of the *t*Bu–C≡C⊃Ag_n ($n=4$ or 5) supramolecular synthon stabilized by silver–ethynide interaction and argentophilicity.[12] The linkage of these silver–ethynide aggregates by trifluoroacetate groups and aqua ligands led to the formation of a relatively rigid 2D coordination network in **1**. Then complexes **2**–**8** were synthesized analogously by adding the corresponding nitrile ligands or quaternary ammonium tetrafluoroborate salts, respectively.

Crystal structures: In the crystal structure of AgC≡C*t*Bu·3 $AgCF_3CO_2$·H_2O (**1**; Figure 1a), the ethynide moiety C1≡C2 (1.213(7) Å) is attached to a butterfly-shaped Ag_4 basket in the μ_4-η^1,η^1,η^1,η^2 mode, which is similar to the coordination mode at each terminal of the $^-$C≡C–C≡C$^-$ dianion.[8af] The distances between the silver atoms range from 2.887(1) to 3.028(1) Å, (less than twice the van der Waals radius of the silver atom: 3.4 Å), suggesting the existence of significant Ag···Ag interaction.[12] Such an Ag_4 basket connects with its inversion-related partner by two trifluoroacetate groups, O5–O6 and O5A–O6A, in an *anti*-μ_3-*O*,*O*′,*O*′ mode (**A**) to produce a silver column along the [010] direction (Figure 1b). These Ag_4 baskets are also linked by bridging trifluoroacetate ligands of the O1–O2 type in the *syn*-μ_3-*O*,*O*′,*O*′ mode (**B**) to form another coordination column along the [100] direction. These two kinds of coordination columns are interwoven to form a honeycomb layer parallel to the (001) plane. Interestingly, each hexagonal-honeycomb cell is a metallacycle composed of six Ag_4 aggregates and four pairs of trifluoroacetate groups, with an inversion center located at the center of each boundary. The CF_3 moieties and *tert*-butyl groups protrude on both sides of this

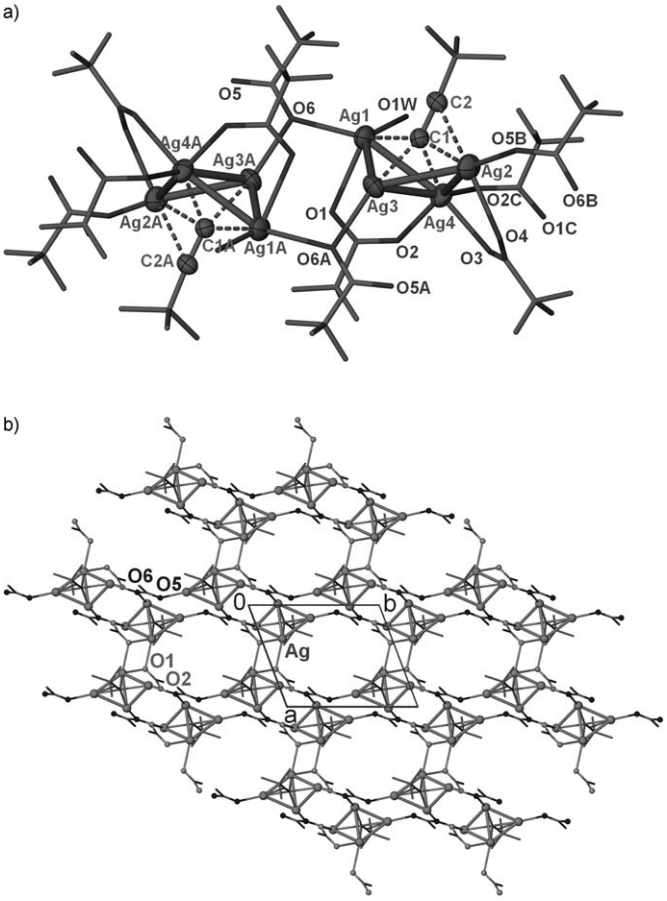

Figure 1. a) Atom labeling (50% thermal ellipsoids) and coordination modes of the *tert*-butylethynide ligands in AgC≡C*t*Bu·3 $AgCF_3CO_2$·H_2O (**1**). Other ligands are omitted for clarity. Symmetry code: A $-x,-y,1-z$; B $x,1+y,z$; C $1-x,-y,1-z$. b) Layer structure in complex **1** composed of a hexagonal array of fused macrocycles; each macrocycle consists of six Ag_4 aggregates connected by two types of O1–O2 (gray) and O5–O6 (black) trifluoroacetate groups. All hydrogen atoms, fluorine atoms, water molecules, and other trifluoroacetate groups are omitted for clarity.

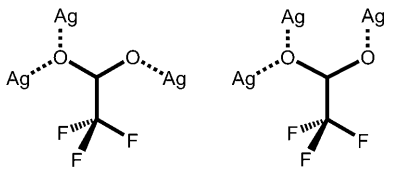

A *anti*-bridging mode **B** *syn*-bridging mode

layer to prevent further linkage, whereas packing of these honeycomb layers yields a series of 1.3×1.1 nm channels along the *c* direction (Figure 1b).

Upon addition of acetonitrile in the course of crystallization, the coordination skeleton of the ethynide moiety transforms from μ_4 in **1** to a novel μ_5-$\eta^1,\eta^1,\eta^1,\eta^1,\eta^2$ mode in the crystal structure of $AgC{\equiv}CtBu{\cdot}5\,AgCF_3CO_2{\cdot}4\,CH_3CN{\cdot}H_2O$ (**2**), in which Ag5 bearing two nitrile ligands (N3 and N4) is attached to the butterfly-shaped Ag_4 basket surrounding the ethynide moiety C1≡C2 to constitute an approximately square-pyramidal Ag_5 aggregate (Figure 2a). Another nitrile-bonded silver atom, Ag6, exhibiting tetrahedral coordination geometry connects with this Ag_5 aggregate through the linkage of two trifluoroacetate groups (O1–O2 and O7–O8) through a *syn*-μ_3-*O*,*O*′,*O*′ mode **B**, thus generating a hexanuclear silver–ethynide–carboxylate cluster. Such hexanuclear segments are further bridged pairwise by inversion-related trifluoroacetate groups O3–O4 and O3A–O4A, also through *syn* ligation mode **B**, to produce a discrete Ag_6-(μ_3-*O*,*O*′,*O*′−$CF_3CO_2)_2$−Ag_6 structural unit. This unit is reminiscent of that observed in our previously reported complex $AgC{\equiv}CtBu{\cdot}6\,AgCF_3CO_2{\cdot}2\,CH_3CN{\cdot}6\,H_2O$,[8c] wherein less acetonitrile was added to the crystallization solution. Linkage of these discrete units by two hydrogen bonds (O1W–O3 2.824 Å and O1W–O9 2.806 Å) engenders a column along the *b* direction, which is further connected by relatively weak hydrogen bonds C20–H···O6 (H···O 2.409 Å) along the *c* direction to yield a hydrogen-bonded layer parallel to the *bc* plane (Figure 2b).

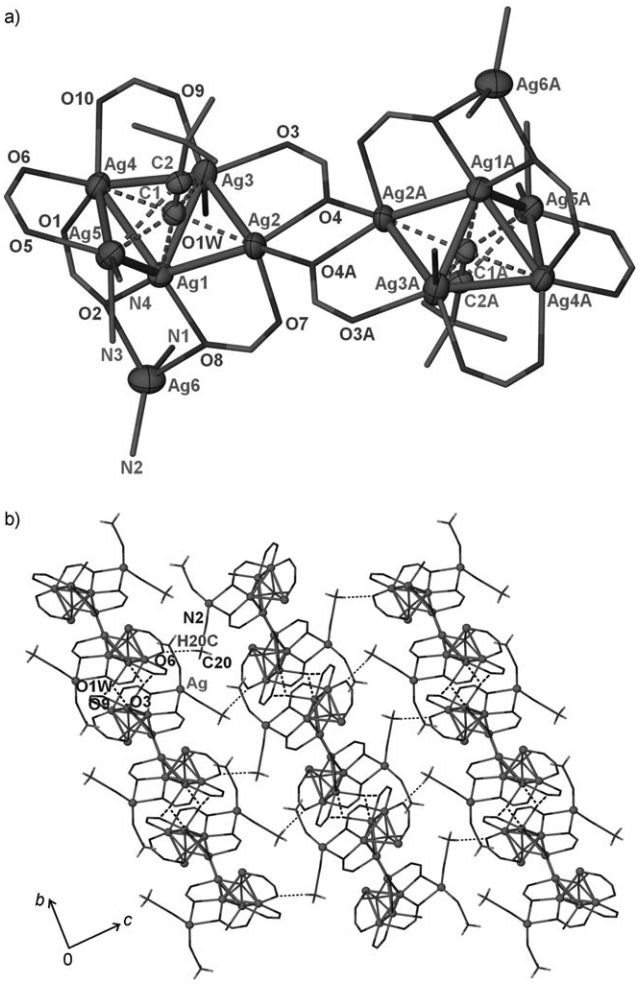

Figure 2. a) Atom labeling (50% thermal ellipsoids) and discrete Ag_6–(μ_3-*O*,*O*′,*O*′-$CF_3CO_2)_2$–Ag_6 structural unit in $AgC{\equiv}CtBu{\cdot}5\,AgCF_3CO_2{\cdot}4\,CH_3CN{\cdot}H_2O$ (**2**). All hydrogen atoms, CF_3 moieties, and methyl groups of acetonitrile are omitted for clarity. Symmetry code: A $1-x,1-y,-z$. Selected bond distances (Å): C1–C2 1.191(7), Ag···Ag 2.875(1)–3.065(1). b) Layer interwoven by hydrogen bonding along the *b* and *c* directions.

A μ_5 coordination mode for the ethynide moiety C1≡C2 similar to that in **2** is also observed in $AgC{\equiv}CtBu{\cdot}3\,AgCF_3CO_2{\cdot}CH_3CH_2CN{\cdot}2\,H_2O$ (**3**), although the more bulky propionitrile ligand is employed in crystallization. Notably, pairs of such *t*BuC≡C⊃Ag_5 aggregates approach each other so that they coalesce by sharing one slant edge Ag2···Ag2A to generate a centrosymmetric octanuclear silver segment (Figure 3a) with a propionitrile ligand appended to each Ag4. This octanuclear silver segment is further stabilized by bridging trifluoroacetate groups (O5–O6 and O5A–O6A), and consecutive O1–O2 linkage by trifluoroacetate groups in the *anti*-μ_3-η^1,η^2 mode produces a coordination silver column along the [100] direction. Subsequently, the strong hydrogen bonds between the water molecule O2W and the oxygen atoms of two trifluoroacetate groups (O3–O4 and O5–O6) crosslink adjacent coordination silver columns, resulting in the formation of a (4,4) network parallel to the *ab* plane (Figure 3b).

When the bulkier ancillary ligand *t*BuC≡N is employed, two Ag_5 aggregates around a pair of proximal ethynide moieties in $AgC{\equiv}CtBu{\cdot}4\,AgCF_3CO_2{\cdot}(CH_3)_3CCN{\cdot}2\,H_2O$ (**4**) approach each other and consequently merge to form an octanuclear silver aggregate by sharing one square edge (Figure 4a), in comparison with square-pyramidal edge-sharing in complex **3**. Each peripheral Ag···Ag edge of this Ag_8 aggregate is spanned by one trifluoroacetate ligand except for Ag1, whose appended *tert*-butyronitrile ligand blocks ligation of the trifluoroacetate group. Ag5 is attached to such an octanuclear aggregate through the connection of two trifluoroacetate groups of the O3–O4 and O5–O6 type in the *syn*-μ_3-η^1,η^2 mode. Furthermore, the Ag_8 aggregates each bearing two *tert*-butylethynide ligands are linked by trifluoroacetate groups of the O7–O8 type and the [Ag_2(μ_2-$CF_3CO_2)_2$] bridging unit (constructed from the external silver atom Ag5 and the O1–O2 trifluoroacetate group) to form a (4,4) coordination network parallel to the *ac* plane (Figure 4b).

Considering the consistent appearance of a layer structure in $AgC{\equiv}CtBu{\cdot}n\,AgCF_3CO_2$ double salt systems (see above), we subsequently introduced various quaternary ammonium ions as guest templates in the expectation that they would play significant roles in affecting the formation of the host framework. In the crystal structure of $AgC{\equiv}CtBu{\cdot}4\,AgCF_3CO_2{\cdot}(BnMe_3N)(CF_3CO_2){\cdot}2\,H_2O$ (**5**), the ethynide moiety C1≡C2 (1.207(7) Å) adopting a μ_5-$\eta^1,\eta^1,\eta^1,\eta^1,\eta^2$

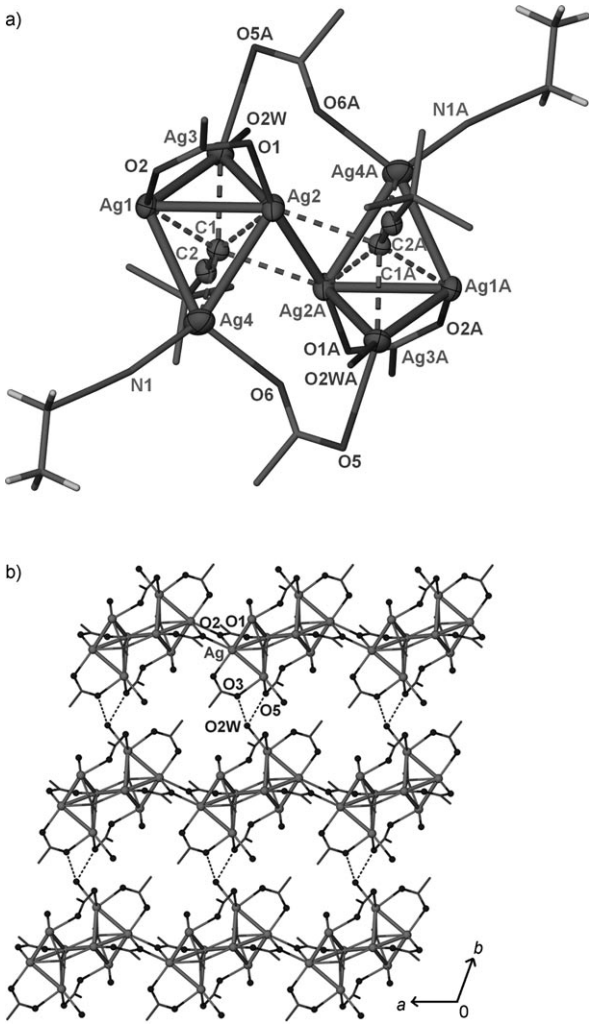

Figure 3. a) Atom labeling (40% thermal ellipsoids) and two edge-shared Ag_5 aggregates in $AgC{\equiv}CtBu{\cdot}3\,AgCF_3CO_2{\cdot}CH_3CH_2CN{\cdot}2\,H_2O$ (**3**). Some hydrogen atoms and CF_3 moieties are omitted for clarity. Symmetry code: A $-x,1-y,1-z$. Selected bond distances (Å): C1–C2 1.195(9), Ag···Ag 2.808(1)–3.105(1). b) Hybrid (4,4) network in **3** connected by coordination bonds (μ_3-η^1,η^2 O1–O2) along the *a* direction and hydrogen bonds (O5–O2W 2.866 Å and O3–O2W 2.787 Å) along the *b* direction. All hydrogen atoms, *tert*-butyl groups, and CF_3 groups are omitted for clarity.

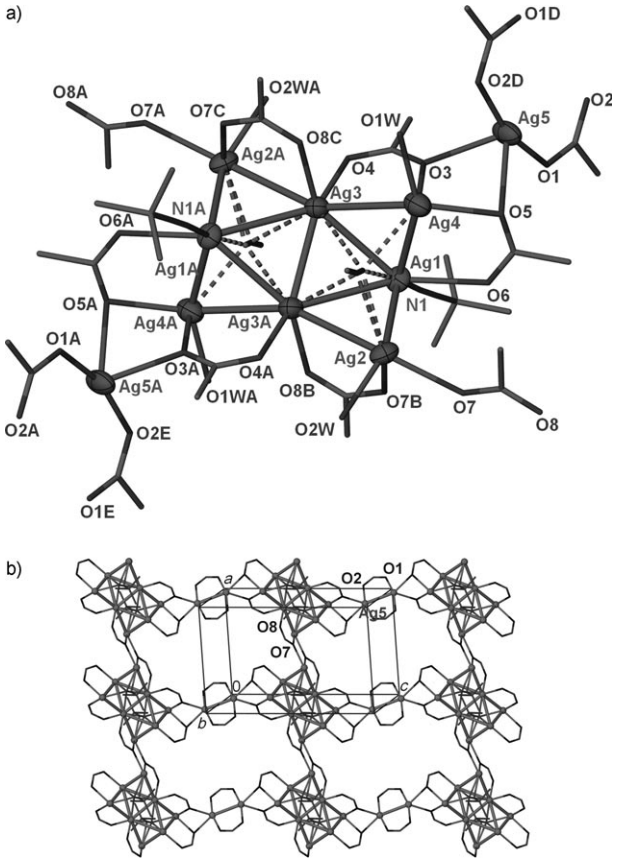

Figure 4. a) Atom labeling (50% thermal ellipsoids) in $AgC{\equiv}CtBu{\cdot}4\,AgCF_3CO_2{\cdot}(CH_3)_3CCN{\cdot}2\,H_2O$ (**4**) and linkage of trifluoroacetate groups around the centrosymmetric Ag_8 aggregate. Other ligands or atoms are omitted for clarity. Symmetry code: A $-x,1-y,1-z$; B $1-x,1-y,1-z$; C $x-1,y,z$; D $-x,1-y,-z$; E $x,y,1+z$. Selected bond distances (Å): C1–C2 1.219(5), Ag···Ag 2.848(1)–3.151(1). b) (4,4) coordination network in **4** linked by trifluoroacetate groups O7–O8 and [$Ag_2(\mu_2$-$CF_3CO_2)_2$] bridging units to form a (4,4) coordination network parallel to the *ac* plane. All hydrogen atoms, *tert*-butyl groups, and CF_3 moieties are omitted for clarity.

coordination mode is still enveloped in a square-pyramidal Ag_5 basket (Figure 5a), in which the Ag···Ag distances range from 2.807(1) to 3.092(1) Å. Except for the μ_3 O7–O8 trifluoroacetate group, each other trifluoroacetate group spans an Ag···Ag edge through the μ_2 mode. Two such Ag_5 baskets are bridged by inversion-related trifluoroacetate groups (O7–O8 and O7A–O8A) to generate an Ag_5-(μ_3-η^1,η^2-$CF_3CO_2)_2$–Ag_5 building unit. These building units are further linked by hydrogen bonds between O1W and two CF_3CO_2 groups (O1–O2 and O9–O10), and between O2W and the other two (O3–O4 and O5–O6), to generate a 2D hydrogen-bonded network parallel to the (010) plane (Figure 5b)). Herein, all *tert*-butyl moieties are located within the plane of the 2D hydrogen-bonded network, in sharp contrast to the 2D networks in **1**–**4** with *tert*-butyl species sticking almost vertically out of the plane. This difference mostly results from steric hindrance of the included quaternary ammonium cations.

The 2D hydrogen-bonded networks are stacked layer by layer along the *b* direction, with an interlayer separation of 13.970 Å. The $BnMe_3N^+$ guests that are accommodated in the interstices between adjacent networks are stabilized by a series of weak C–H···O and C–H···F hydrogen bonds between the alkyl moieties of quaternary ammonium cations and trifluoroacetate groups (Figure 6).

A totally identical layer-type host lattice also exists in the crystal structures of $AgC{\equiv}CtBu{\cdot}4\,AgCF_3CO_2{\cdot}(Et_4N)$-$(CF_3CO_2){\cdot}2\,H_2O$ (**6**) and $AgC{\equiv}CtBu{\cdot}4\,AgCF_3CO_2{\cdot}(nPr_4N)$-$(CF_3CO_2){\cdot}2\,H_2O$ (**7**), which can be properly described as isostructural complexes of **5**. Notably, the separation between adjacent hydrogen-bonded layers can be tuned by varying the bulk of the hydrophobic organic cations. With the increase in steric volume of quaternary ammonium cations in

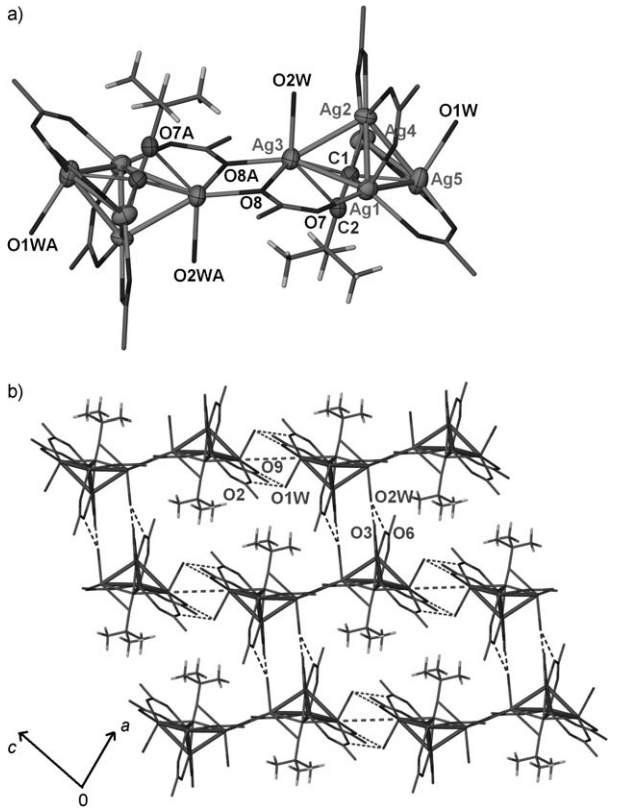

Figure 5. a) Atom labeling (50% thermal ellipsoids) of AgC≡C*t*Bu·4 $AgCF_3CO_2$·($BnMe_3N$)(CF_3CO_2)·2 H_2O (**5**) and two carboxylate-bridged Ag_5 aggregates. Other ligands are omitted for clarity. Symmetry code: A $-x,1-y,1-z$. b) 2D hydrogen bonding network in **5**. Hydrogen bond distances (Å): O1W–O2 2.799, O1W–O9 2.806, O2W–O3 2.829, O2W–O6 2.777. All fluorine atoms and $BnMe_3N^+$ cations are omitted for clarity.

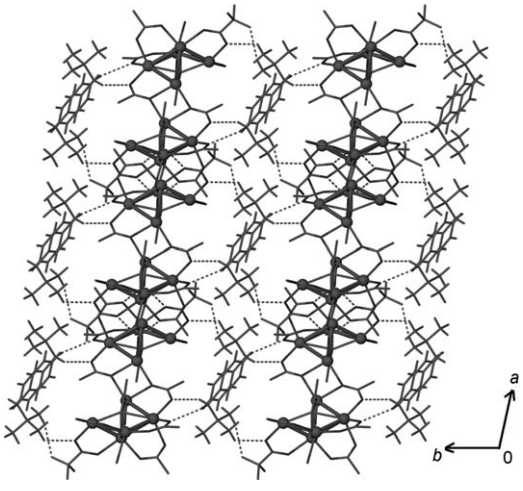

Figure 6. Packing of hydrogen-bonded layers, which are separated by $BnMe_3N^+$ ions, in the crystal structure of **5**. Other ligands are omitted for clarity.

the order $BnMe_3N < Et_4N < nPr_4N$, the corresponding interlayer separation changes from 13.970 Å through 15.075 Å to 15.143 Å.

Further extending the alkyl chain length by introducing nBu_4N^+ into the system, we eventually arrive at a packing of discrete molecular moieties in AgC≡C*t*Bu·4 $AgCF_3CO_2$·3[(nBu_4N)(CF_3CO_2)]·H_2O (**8**), in which the bulky cations totally interrupt the 2D hydrogen-bonding network (Figure 7b). The Ag_5 aggregate surrounding the ethynide moiety

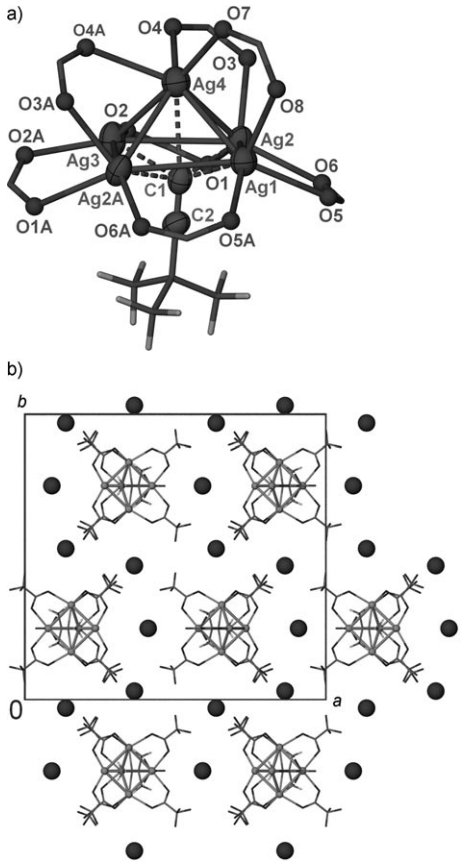

Figure 7. a) Perspective drawing (40% possibility) of *nido*-Ag_5 aggregate in AgC≡C*t*Bu·4 $AgCF_3CO_2$·3[(nBu_4N)(CF_3CO_2)]·H_2O (**8**). b) Packing of discrete molecular species viewed along the *c* direction. The black circles indicate the nBu_4N moieties.

C1≡C2 (1.168(15) Å) in **8** exhibits a kind of closed *nido*-square-pyramidal cage structure with Ag···Ag square edges ranging from 3.118(1) to 3.174(1) Å, which differs greatly from the reported Ag_5 aggregates of *t*BuC≡C$^-$ or PhC≡C$^-$ ligands[8c,d] with a trapeziform four-membered base (Figure 7a). Although the ethynide moiety is located about 0.66 Å outside the Ag_4 square base and the C1–Ag4 bond length (2.31(1) Å) is much longer than the congener bond length of 2.1–2.2 Å in **1**–**7**, this closed *nido*-Ag_5 cluster is still stabilized by as many as seven trifluoroacetate groups by bridging the Ag···Ag edges. This is analogous to one half of the previously reported bicapped square-antiprismatic $C_2@Ag_{10}$ aggregate, the largest discrete ethynide-encapsulating silver cage stabilized by eleven trifluoroacetate groups and two 4-hydroxyquinoline ligands.[13]

There are three independent nBu$_4$N$^+$ ions in the asymmetric unit. Packing of the discrete $[Ag_5(C{\equiv}Ct\text{Bu})(CF_3CO_2)_7(H_2O)]^{3-}$ and nBu$_4$N$^+$ ions is shown in Figure 7b.

Effect of nitrile ligands: The coordination skeletons and 2D networks observed in **1**–**4** lead to the following generalizations.

1) With the addition of different nitrile groups, two Ag_n ($n=4$ or 5) aggregates approach mutually and eventually merge together by sharing one vertex or one edge. Table 1 lists the separations of the two nearest *tert*-butylethynide moieties on one side (defined by the distance between their terminal carbon atoms) in **1**–**4**, which vary in accordance with the transformation of linkage mode between two Ag_n ($n=4$ or 5) aggregates from carboxylate-bridged to edge-shared.
2) The nitrile-bonded silver atom changes its role from being peripheral in **2**, through basal in **3**, to apical in **4**, which to some extent reflects the relative crowding around the tBu-C≡C⊃Ag$_5$ supramolecular synthon.
3) On addition of the acetonitrile ligand, some coordination bonds of the 2D network in **1** are broken, and the expanded 2D network in **2** is totally linked by hydrogen bonds; this can be explained by the fact that nitrile ligands always bond to a peripheral silver atom of tBu−C≡C⊃Ag$_n$ ($n=4$, 5) and sterically prevent the linkage of carboxylate ligands ($CF_3CO_2^-$) from forming a higher-dimensional coordination network. Coordination by bulkier and more hydrophobic nitrile ligands, such as CH_3CH_2CN in **3** and $(CH_3)_3CCN$ in **4**, further hinders the proximal approach of the trifluoroacetate groups and water molecules. This causes two Ag_5 aggregates in **4** to condense into one Ag_8 aggregate by sharing one common Ag···Ag edge, which leads to reduction of the number of trifluoroacetate groups required for charge balance. On the other hand, silver trifluoroacetate moieties that are expelled from the coordination sphere of the ethynide-encapsulating silver aggregate by the bulky nitrile groups spontaneously constitute $[Ag_2(\mu_2\text{-}CF_3CO_2)_2]$ bridging units to link the aforementioned congregated Ag_8 segments to re-form a 2D coordination network. Consequently, variation of the bulkiness of ancillary terminal nitrile ligands leads to successive realization of a 2D coordination network in **1**, a hydrogen-bonded 2D network in **2**, a hybrid coordination/hydrogen-bonded 2D network in **3**, and a new 2D coordination network in **4**.

Role played by quaternary ammonium cations: In contrast to reported host–guest complexes mostly composed of hydrogen-bonded organic compounds with quaternary ammonium ions serving as guest templates for charge balance and space filling,[14] the 2D host network in **5**–**7** is constructed through the linkage of carboxylate-bridged Ag_5−$(\mu_3\text{-}\eta^1,\eta^2\text{-}CF_3CO_2)_2$−$Ag_5$ building units by a series of hydrogen bonds, the integrity of which can be maintained in the presence of quaternary ammonium cations from $BnMe_3N^+$ through Et_4N^+ to nPr$_4$N$^+$. The separation between adjacent layers in the host network can be tuned by varying the bulk of the hydrophobic organic cations. However, disruption of this host–guest structure in complex **8** is achieved by introducing the bulkier spectator cation nBu$_4$N$^+$ into the system. This can be rationalized by the premise that when the interlayer separation of the hydrogen-bonded host network increases sufficiently, additional trifluoroacetate groups can approach and bind to the tBu−C≡C⊃Ag$_n$ ($n=4$, 5) aggregate to generate a discrete dense *nido*-Ag_5 cluster.

Table 1. The separation of the two nearest *tert*-butylethynide moieties on one side (S) in **1**–**4** and linkage mode transformation.

Complex	**1**	**2**	**3**	**4**
S [Å]	7.14	7.84	3.98	3.99
linkage mode	bridged by $CF_3CO_2^-$ groups	bridged by $CF_3CO_2^-$ groups	pyramidal edge shared	square edge shared

Conclusion

Through synthetic and structural characterization of a series of eight silver(I) complexes containing *tert*-butylethynide and trifluoroacetate, we have established a general methodology to construct coordination and hydrogen-bonded networks through the metal–ligand supramolecular synthon tBuC≡C⊃Ag$_n$ ($n=4$, 5). The influence of the bulk of ancillary terminal nitrile ligands on the coordination environment of the ethynide moiety and the resulting network structure was also investigated, leading to transformation from a 2D coordination network in **1**, through a hydrogen-bonded 2D network in **2**, to a hybrid coordination/hydrogen-bonded 2D network in **3**, and eventually to a new 2D coordination network in **4**. This approach offers a viable means of controlling the crystallization process other than those involving conventional metal–ligand factors. Moreover, investigation of the inclusion behavior of the layer-type hydrogen-bonded host lattice in isostructural complexes **5**–**7** generated by quaternary ammonium cations as guest templates indicates that a high degree of tunability of the interlayer separation can be realized by varying the bulk of the entrapped spectator cations up to a critical limit, beyond which the network transforms to zero-dimensional as observed in complex **8**.

Experimental Section

Reagents: 3,3-Dimethylbut-1-yne (Alfa Aesar, >98%) and *n*-BuLi in hexane (Merck, 1.6 M) were available commercially and used without further purification. Tetrahydrofuran (THF) was purified by refluxing over sodium and benzophenone. All other reagents were of analytical grade and used as received. Infrared spectra were obtained from KBr pellets on a Nicolet Impact 420 FTIR spectrometer in the 400–4000 cm^{-1} region.

Elemental analysis (C,H,N) was performed by the Medac Ltd Brunel Science Center, UK.

CAUTION! Silver–ethynide complexes are potentially explosive and should be handled with care and in small amounts.

$[AgC{\equiv}CtBu]_n$: In a 100 mL Schlenk flask, THF (20 mL) was cooled to −78 °C in a cold bath. Then *n*BuLi (1.6 M in *n*-hexane, 4.4 mmol) was added through a syringe, and the mixture was stirred for 15 min at −78 °C. A solution of 3,3-dimethylbut-1-yne (0.329 g, 4.0 mmol) dissolved in THF (5 mL) was added dropwise. The cold bath was then replaced by an ice-water bath and the mixture was stirred for 2 h. Under a stream of nitrogen, $AgNO_3$ crystals (0.680 g, 4.0 mmol) were added to the flask and dissolved gradually while the mixture was stirred overnight. A white precipitate of crude $[AgC{\equiv}CtBu]_n$ was isolated by filtration, washed several times with THF, and finally with de-ionized water. Yield: 0.524 g (69.3 %); IR (KBr): $\tilde{\nu}=2056\ cm^{-1}$ (m, C≡C).

$AgC{\equiv}CtBu{\cdot}3AgCF_3CO_2{\cdot}H_2O$ (1): $AgCF_3CO_2$ (0.220 g, 1 mmol) and $AgBF_4$ (0.382 g, 2 mmol) were dissolved in deionized water (1 mL). $[AgC{\equiv}CtBu]_n$ (≈0.1 g) was added to the solution, which was then stirred for about 5 min, filtered off, and placed in the ambient environment for evaporation. After one week, colorless crystals of **1** were collected. Yield ≈30 %; dec. > 115 °C; IR (KBr): $\tilde{\nu}=2008\ cm^{-1}$ (m, C≡C); elemental analysis calcd (%) for $C_{12}H_{11}F_9O_7Ag_4$: C 16.57, H 1.27; found: C 16.44, H 0.93.

$AgC{\equiv}CtBu{\cdot}5AgCF_3CO_2{\cdot}4CH_3CN{\cdot}H_2O$ (2): $[AgC{\equiv}CtBu]_n$ (≈0.1 g) was added to concentrated aqueous solution (1 mL) of $AgCF_3CO_2$ (0.224 g, 1 mmol) and $AgBF_4$ (0.383 g, 2 mmol) in a beaker with stirring until saturation. The excess $[AgC{\equiv}CtBu]_n$ was filtered off. Acetonitrile (0.1 mL) was added to the filtrate, then the solution was placed in the ambient environment for evaporation. After a few days, colorless crystals of **2** were collected. Yield ≈35 %; m.p. 62.6–64.7 °C; IR: $\tilde{\nu}=2013\ cm^{-1}$ (vw, C≡C); elemental analysis (%) for $C_{24}H_{23}F_{15}O_{11}N_4Ag_6$: found: C 19.84, H 1.68, N 3.57; calcd: C 19.53, H 1.57, N 3.80.

$AgC{\equiv}CtBu{\cdot}3AgCF_3CO_2{\cdot}CH_3CH_2CN{\cdot}2H_2O$ (3) and $AgC{\equiv}CtBu{\cdot}4AgCF_3CO_2{\cdot}(CH_3)_3CCN{\cdot}2H_2O$ (4): The method of synthesis was similar to that for complex **2**, but employed propionitrile and *tert*-butylnitrile, respectively, instead of acetonitrile. Compound **3**: m.p. 52.7–54.2 °C; IR: $\tilde{\nu}=2017\ cm^{-1}$ (m, C≡C); elemental analysis (%) for $C_{15}H_{18}F_9O_8NAg_4$: found: C 19.43, H 1.53, N 1.20; calcd: C 19.11, H 1.92, N 1.48. Compound **4** had a melting point ranging from 75.1 to 76.3 °C. IR (KBr): $\tilde{\nu}=2010\ cm^{-1}$ (vw, C≡C); elemental analysis calcd (%) for $C_{19}H_{22}F_{12}O_{10}NAg_5$: C 19.15, H 1.61, N 1.18; found: C 19.05, H 1.86, N, 0.92.

$AgC{\equiv}CtBu{\cdot}4AgCF_3CO_2{\cdot}(BnMe_3N)(CF_3CO_2){\cdot}2H_2O$ (5): $AgCF_3CO_2$ (0.220 g, 1 mmol) and $AgBF_4$ (0.382 g, 2 mmol) were dissolved in deionized water (1 mL). Then $[AgC{\equiv}CtBu]_n$ (≈0.1 g) and $(BnMe_3N)BF_4$ (≈0.1 g) were added to the solution, respectively. After the solution had been stirred for about 10 min, the excess $(BnMe_3N)BF_4$ was filtered off, and the solution was placed in the ambient environment for evaporation. After a few days, colorless crystals of **5** were collected. Yield ≈20 %; m.p. 81.8–82.7 °C. IR (KBr): $\tilde{\nu}=2008\ cm^{-1}$ (vw, C≡C); elemental analysis calcd (%) for $C_{26}H_{29}F_{15}O_{12}NAg_5$: C 22.76, H 2.13, N 1.02; found: C 22.98, H 1.94, N 0.80.

$AgC{\equiv}CtBu{\cdot}4AgCF_3CO_2{\cdot}(Et_4N)(CF_3CO_2){\cdot}2H_2O$ (6), $AgC{\equiv}CtBu{\cdot}4AgCF_3CO_2{\cdot}(nPr_4N)(CF_3CO_2){\cdot}2H_2O$ (7), and $AgC{\equiv}CtBu{\cdot}4AgCF_3CO_2{\cdot}3[(nBu_4N)(CF_3CO_2)]{\cdot}H_2O$ (8): These were obtained by similar methods of synthesis to **5**, but utilizing $(Et_4N)BF_4$, $(nPr_4N)BF_4$ and $(nBu_4N)BF_4$, respectively, instead of $(BnMe_3N)BF_4$.

Compound **6** melted from 97.6 to 98.7 °C. IR (KBr): $\tilde{\nu}=2009\ cm^{-1}$ (vw, C≡C); elemental analysis calcd (%) for $C_{24}H_{33}F_{15}O_{12}NAg_5$: C 21.32, H 2.46, N 1.04; found: C 21.40; H 2.18; N 0.89.

Compound **7** had a melting point ranging from 76.9 to 78.2 °C. IR (KBr): $\tilde{\nu}=2006\ cm^{-1}$ (vw, C≡C); elemental analysis calcd (%) for $C_{28}H_{41}F_{15}O_{12}NAg_5$: C 23.89, H 2.94, N 0.99; found: C 23.74, H 3.21, N 0.83.

Compound **8** melted in the range 90.2 to 91.7 °C. IR (KBr): $\tilde{\nu}=2006\ cm^{-1}$ (m, C≡C); elemental analysis calcd (%) for $C_{68}H_{119}F_{21}O_{15}N_3Ag_5$: C 37.86, H 5.56, N 1.95; found: C 37.42, H 5.40, N 1.80.

X-ray crystallographic analysis: Data for complexes **1–8** were collected at 293 K with $Mo_{K\alpha}$ radiation on a Bruker SMART 1000 CCD diffractometer with frames of oscillation range 0.3°. During data reduction, an empirical absorption correction was applied using the SADABS program.[15] All structures were solved by direct methods, and non-hydrogen atoms were located from difference Fourier maps. All non-hydrogen atoms, unless otherwise noted, were subjected to anisotropic refinement by full-matrix least-squares on F^2 using the SHELXTL program.[16] The parame-

Table 2. Crystallographic data of compounds **1–8**.

Compound	**1**	**2**	**3**	**4**
formula	$C_{12}H_{11}F_9O_7Ag_4$	$C_{24}H_{23}F_{15}O_{11}N_4Ag_6$	$C_{15}H_{18}F_9O_8NAg_4$	$C_{19}H_{22}F_{12}O_{10}NAg_5$
formula wt.	869.67	1475.67	942.75	1191.69
crystal system	triclinic	monoclinic	triclinic	triclinic
space group	$P\bar{1}$	$P2_1/c$	$P\bar{1}$	$P\bar{1}$
a [Å]	9.150(1)	15.600(1)	9.957(3)	9.924(1)
b [Å]	10.815(1)	11.119(1)	11.438(3)	11.526(1)
c [Å]	12.026(1)	25.696(2)	13.168(4)	15.604(2)
α [°]	81.705(2)	90	111.976(3)	109.782(2)
β [°]	76.977(2)	106.189(1)	105.137(3)	95.015(2)
γ [°]	68.048(2)	90	101.157(3)	90.565(2)
V [Å^3]	1073.1(2)	4280.5(5)	1269.4(6)	1671.6(3)
Z	2	4	2	2
ρ_c [g cm^{-3}]	2.685	2.287	2.456	2.360
μ [mm^{-1}]	3.074	2.809	3.145	2.990
R_1[a] ($I>2\sigma$)	0.0331	0.0349	0.0393	0.0324
wR_2[b] (all data)	0.0876	0.0896	0.1088	0.0983
GOF	1.050	1.035	1.026	1.106
	5	**6**	**7**	**8**
formula	$C_{26}H_{29}F_{15}O_{12}NAg_5$	$C_{24}H_{33}F_{15}O_{12}NAg_5$	$C_{28}H_{41}F_{15}O_{12}NAg_5$	$C_{68}H_{119}F_{21}O_{15}N_3Ag_5$
formula wt.	1371.82	1351.83	1407.94	2157.00
crystal system	triclinic	triclinic	triclinic	orthorhombic
space group	$P\bar{1}$	$P\bar{1}$	$P\bar{1}$	*Pnma*
a [Å]	10.449(2)	10.198(1)	10.394(1)	26.905(3)
b [Å]	14.109(2)	14.492(2)	14.488(2)	25.495(3)
c [Å]	14.447(2)	15.666(2)	15.259(2)	13.836(2)
α [°]	88.877(3)	107.575(2)	97.042(2)	90
β [°]	82.121(3)	105.789(2)	96.745(2)	90
γ [°]	81.972(3)	96.712(2)	97.298(2)	90
V [Å^3]	2089.0(5)	2073.4(4)	2241.3(4)	9491(2)
Z	2	2	2	4
ρ_c [g cm^{-3}]	2.175	2.127	2.080	1.508
μ [mm^{-1}]	2.422	2.437	2.260	1.108
R_1[a] ($I>2\sigma$)	0.0430	0.0487	0.0440	0.0594
wR_2[b] (all data)	0.1180	0.1400	0.1240	0.2288
GOF	1.013	1.023	1.011	0.989

[a] $R_1=\Sigma||F_o|-|F_c||/\Sigma|F_o|$. [b] $wR_2=\{\Sigma[w(F_o^2-F_c^2)^2]/\Sigma[w(F_o^2)^2]\}^{1/2}$.

ters for the crystal data and X-ray structure analysis are summarized in Table 2. The refinement details are described in the Supporting Information. CCDC-679283 (**1**), 679284 (**2**), 679285 (**3**), 679286 (**4**), 679287 (**5**), 679288 (**6**), 679289 (**7**), and 679290 (**8**) contain the supplementary crystallographic data for this paper. These data can be obtained free of charge from The Cambridge Crystallographic Data Centre via www.ccdc.cam.ac.uk/data_request/cif.

Acknowledgement

This work is supported by the Hong Kong Research Grants Council (CERG Ref. No. Earmarked Grant CUHK 402405) and The Chinese University of Hong Kong (postdoctoral fellowship awarded to X.-D. Chen).

[1] a) N. J. Long, *Angew. Chem.* **1995**, *107*, 37–56; *Angew. Chem. Int. Ed. Engl.* **1995**, *34*, 21–38; b) S. Barlow, D. O'Hare, *Chem. Rev.* **1997**, *97*, 637–669; c) I. R. Whittal, A. M. McDonagh, M. G. Humphrey, *Adv. Organomet. Chem.* **1998**, *42*, 291–362; d) M. P. Cifuentes, M. G. Humphrey, *J. Organomet. Chem.* **2004**, *689*, 3968–3981.

[2] a) M. J. Irwin, J. J. Vittal, R. J. Puddephatt, *Organometallics* **1997**, *16*, 3541–3547; b) M. Younus, A. Kohler, S. Cron, N. Chawdhury, M. R. A. Al-Madani, M. S. Khan, N. J. Long, R. H. Friend, P. R. Raithby, *Angew. Chem.* **1998**, *110*, 3180–3183; *Angew. Chem. Int. Ed.* **1998**, *37*, 3036–3039; c) V. W.-W. Yam, K. K.-W. Lo, K. M.-C. Wong, *J. Organomet. Chem.* **1999**, *578*, 3–30; d) V. W.-W. Yam, *Acc. Chem. Res.* **2002**, *35*, 555–563; e) K.-L. Cheung, S.-K. Yip, V. W.-W. Yam, *J. Organomet. Chem.* **2004**, *689*, 4451–4462.

[3] a) F. Paul, C. Lapinte, *Coord. Chem. Rev.* **1998**, *178–180*, 431–509; b) M. I. Bruce, P. J. Low, *Adv. Organomet. Chem.* **2004**, *50*, 179–444; c) V. W.-W. Yam, K. M.-C. Wong, *Top. Curr. Chem.* **2005**, *257*, 1–32; d) S. Rigaut, C. Olivier, K. Costuas, S. Choua, O. Fadhel, J. Massue, P. Turek, J. Y. Saillard, P. H. Dixneuf, D. Touchard, *J. Am. Chem. Soc.* **2006**, *128*, 5859–5876.

[4] a) S. Lotz, P. H. van Rooyen, R. Meyer, *Adv. Organomet. Chem.* **1995**, *37*, 219–320; b) V. W.-W. Yam, W. K.-M. Fung, K.-K. Cheung, *Angew. Chem.* **1996**, *108*, 1213–1215; *Angew. Chem. Int. Ed. Engl.* **1996**, *35*, 1100–1102; c) S. Yamazaki, *Recent Res. Dev. Pure Appl. Chem.* **1998**, *2*, 401–426; d) C. P. McArdle, J. J. Vittal, R. J. Puddephatt, *Angew. Chem.* **2000**, *112*, 3977–3980; *Angew. Chem. Int. Ed.* **2000**, *39*, 3819–3822; e) P. J. Low, M. I. Bruce, *Adv. Organomet. Chem.* **2001**, *48*, 71–286; f) N. J. Long, C. K. Williams, *Angew. Chem.* **2003**, *115*, 2690–2722; *Angew. Chem. Int. Ed.* **2003**, *42*, 2586–2617; g) G. T. Dalton, L. Viau, S. M. Waterman, M. G. Humphrey, M. I. Bruce, P. J. Low, R. L. Roberts, A. C. Willis, G. A. Koutsantonis, B. W. Skelton, A. H. White, *Inorg. Chem.* **2005**, *44*, 3261–3269.

[5] J. Manna, K. D. John, M. D. Hopkins, *Adv. Organomet. Chem.* **1995**, *38*, 79–154.

[6] a) J. Fornies, S. Fuertes, A. Martin, V. Sicilia, E. Lalinde, M. T. Moreno, *Chem. Eur. J.* **2006**, *12*, 8253–8266; b) A. B. Antonova, M. I. Bruce, P. A. Humphrey, M. Gaudio, B. K. Nicholson, K. Brian, N. Scoleri, B. W. Skelton, A. H. White, N. N. Zaitseva, *J. Organomet. Chem.* **2006**, *691*, 4694–4707; c) C. W. Baxter, T. C. Higgs, P. J. Bailey, S. Parsons, F. McLachlan, M. McPartlin, P. A. Tasker, *Chem. Eur. J.* **2006**, *12*, 6166–6174; d) M. I. Bruce, P. A. Humphrey, M. Jevric, G. J. Perkins, B. W. Skelton, A. H. White, *J. Organomet. Chem.* **2007**, *692*, 1748–1756.

[7] a) M. G. Humphrey, D. M. P. Mingos, *J. Organomet. Chem.* **2003**, *670*, 1–264 (special issue); b) W.-Y. Wong, *Coord. Chem. Rev.* **2007**, *251*, 2400–2427.

[8] a) L. Zhao, T. C. W. Mak, *J. Am. Chem. Soc.* **2004**, *126*, 6852–6853; b) L. Zhao, T. C. W. Mak, *J. Am. Chem. Soc.* **2005**, *127*, 14966–14967; c) L. Zhao, W.-Y. Wong, T. C. W. Mak, *Chem. Eur. J.* **2006**, *12*, 4865–4872; d) L. Zhao, X.-L. Zhao, T. C. W. Mak, *Chem. Eur. J.* **2007**, *13*, 5927–5936; e) T. C. W. Mak, L. Zhao, *Chem. Asian J.* **2007**, *2*, 456–467; f) L. Zhao, M. Du, T. C. W. Mak, *Chem. Asian J.* **2007**, *2*, 1240–1257.

[9] a) H.-X. Zhang, B.-S. Kang, A.-W. Xu, H.-Q. Liu, Z.-N. Chen, *Comments Inorg. Chem.* **2002**, *23*, 231–248; b) V. Balamurugan, W. Jacob, J. Mukherjee, R. Mukherjee, *CrystEngComm* **2004**, *6*, 396–400; c) J. Burgess, J. R. A. Cottam, P. J. Steel, *Aust. J. Chem.* **2006**, *59*, 295–297.

[10] a) M. A. Withersby, A. J. Blake, N. R. Champness, P. Hubberstey, W. S. Li, M. Schröder, *Angew. Chem.* **1997**, *109*, 2421–2423; *Angew. Chem. Int. Ed. Engl.* **1997**, *36*, 2327–2329; b) M. A. Withersby, A. J. Blake, N. R. Champness, P. A. Cooke, P. Hubberstey, W. S. Li, M. Schröder, *Inorg. Chem.* **1999**, *38*, 2259–2266; c) A. J. Blake, N. R. Champness, P. A. Cooke, J. E. B. Nicolson, C. Wilson, *J. Chem. Soc. Dalton Trans.* **2000**, 3811–3819; d) N. P. Chatterton, D. M. L. Goodgame, D. A. Grachvogel, I. Hussain, A. J. P. White, D. J. Williams, *Inorg. Chem.* **2001**, *40*, 312–317; e) S. Noro, R. Kitaura, M. Kondo, S. Kitagawa, T. Ishii, H. Matsuzaka, M. Yamashita, *J. Am. Chem. Soc.* **2002**, *124*, 2568–2583; f) M.-L. Tong, Y.-M. Wu, J. Ru, X.-M. Chen, H.-C. Chang, S. Kitagawa, *Inorg. Chem.* **2002**, *41*, 4846–4848; g) R. P. Feazell, C. E. Carson, K. K. Klausmeyer, *Inorg. Chem.* **2006**, *45*, 2635–2643.

[11] Q.-M. Wang, T. C. W. Mak, *Chem. Commun.* **2000**, 1534–1536.

[12] a) M. Jansen, *Angew. Chem.* **1987**, *99*, 1136–1149; *Angew. Chem. Int. Ed. Engl.* **1987**, *26*, 1098–1110; b) P. Pyykkö, *Chem. Rev.* **1997**, *97*, 597–636; c) M. A. Omary, T. R. Webb, Z. Assefa, G. E. Shankle, H. H. Patterson, *Inorg. Chem.* **1998**, *37*, 1380–1386; d) P. Majumdar, K. K. Kamar, S. Goswami, A. Castineiras, *Chem. Commun.* **2001**, 1292–1293; e) L. Pan, E. B. Woodlock, X. Wang, K.-C. Lam, A. L. Rheingold, *Chem. Commun.* **2001**, 1762–1763; f) H.-B. Song, Z.-Z. Zhang, Z. Hui, C.-M. Che, T. C. W. Mak, *Inorg. Chem.* **2002**, *41*, 3146–3154; g) Y. Yoshida, K. Muroi, A. Otsuka, G. Saito, M. Takahashi, T. Yoko, *Inorg. Chem.* **2004**, *43*, 1458–1462; h) X.-D. Chen, M. Du, T. C. W. Mak, *Chem. Commun.* **2005**, 4417–4419.

[13] X.-L. Zhao, Q.-M. Wang, T. C. W. Mak, *Inorg. Chem.* **2003**, *42*, 7872–7876.

[14] a) T. C. W. Mak, Q. Li in *Advances in Molecular Structure and Research, Vol. 4* (Eds.: M. Hargittai, I. Hargittai), JAI Press, Stamford, CT, **1998**, pp. 151–225; b) T. C. W. Mak, F. Xue, *J. Am. Chem. Soc.* **2000**, *122*, 9860–9861; c) C.-K. Lam, T. C. W. Mak, *Angew. Chem.* **2001**, *113*, 3561–3563; *Angew. Chem. Int. Ed.* **2001**, *40*, 3453–3455; d) C.-K. Lam, F. Xue, J.-P. Zheng, X.-M. Chen, T. C. W. Mak, *J. Am. Chem. Soc.* **2005**, *127*, 11536–11537.

[15] G. M. Sheldrick, SADABS: Program for Empirical Absorption Correction of Area Detector Data, Univ. of Göttingen: Germany, **1996**.

[16] G. M. Sheldrick, SHELXTL 5.10 for Windows NT: Structure Determination Software Programs, Bruker Analytic X-Ray Systems, Inc., Madison, WI, **1997**.

Received: May 21, 2008
Published online: October 8, 2008

